

## Determining Pad-Wafer Contact using Dual Emission Laser Induced Fluorescence

Caprice Gray<sup>1</sup>, Chris Rogers<sup>1</sup>, Vincent P. Manno<sup>1</sup>, Robert White<sup>1</sup>, Mansour Moinpour<sup>2</sup>, and Sriram Anjur<sup>3</sup>

<sup>1</sup>Tufts University, Medford, MA, 02155

<sup>2</sup>Intel Corporation, Santa Clara, CA, 95052

<sup>3</sup>Cabot Microelectronics, Aurora, IL, 60504

### ABSTRACT

It is becoming increasingly clear that understanding the small scale polishing mechanisms operating during CMP requires knowledge of the nature of the pad-wafer contact. Dual Emission Laser Induced Fluorescence (DELIF) can be used to study the fluid layer profile between the polishing pad and the wafer during CMP. Interactions between the polishing pad surface and the wafer can then be deduced from the fluid layer profile. We present a technique and some preliminary data for instantaneous measurement of in-situ pad-wafer contact, defined as the point at which the fluid film thickness goes to zero, using DELIF. The imaging area is 1.30mmx1.74 mm with a resolution of 2.5  $\mu\text{m}/\text{pixel}$ . At this magnification, some regions imaged contain contact, whereas others do not. For the contact regions discussed in this paper, contact percentage varies from 0.07% to 0.27% using a Cabot Microelectronics D100 polishing pad. The asperity contact area increases with applied load, which was varied from 0.28 to 3.1 psi.

### INTRODUCTION

It is beneficial to understand polishing pad-wafer contact during chemical mechanical polishing (CMP) so we can gain insight into the material removal rate (MRR) mechanism during polishing<sup>1</sup>. Integrated circuit manufacturers expend significant effort trying to control MRR during CMP. Manufacturing processes are often determined by trial and error due to incomplete understanding of the polishing mechanisms. One removal mechanism proposed by Cook<sup>2</sup> suggests that the mechanical action of slurry particles can provide additional energy required to break and re-order the chemical bonds on the glass substrate surface so as to significantly increase the MRR. More recently, it has been suggested that the primary mode of transport of slurry particles to the glass surface is via polishing pad asperities that come into contact with the substrate<sup>3</sup>.

The first step in determining pad-wafer contact is to accurately examine the 3D polishing pad topography. There are several standard techniques for attaining 3D topography, some of which include profilometer scanning, laser interferometry and confocal microscopy.

Profilometry provides excellent 3D images, but is not a viable option for observing pad-wafer contact because the technique requires contact of a stylus with the surface being characterized. Optical techniques are more promising for determining contact between a polishing pad and an optical glass disk. Interferometry has been used in tribology to make thin fluid film measurements between an optical glass flat and a steel ball bearing<sup>4</sup>. However interferometry is not a practical technique for measuring contact or fluid films in CMP because the technique requires that the pad be specularly reflective. Confocal reflectance interference contrast microscopy (C-RICM) has recently produced excellent contact images between a sapphire disk and Rohm and Haas IC1000 and VP3000 polishing pads<sup>5</sup>. These measurements were taken outside the polishing setup (ex-situ). Measurements of pad-wafer contact on the IC1000 were between 0-2% for a pressure range of 0-6psi<sup>6</sup>.

Dual Emission Laser Induced Fluorescence (DELIF) has been used to attain high-resolution 3D slurry layer and polishing pad profiles<sup>7</sup> and is capable of measuring instantaneous slurry layer thickness during the polishing process (in-situ)<sup>8</sup>. Previous investigations of pad-wafer interactions using DELIF include in-situ measurements of average fluid layer thickness, asperity layer compressibility, surface roughness measurements and polishing pad rebound into etched wells<sup>9</sup>. The difficulty with fluorescent imaging of fluid films is that both the information about the fluid layer thickness and information about the excitation source are contained in the signal<sup>10</sup>. In DELIF, there are two fluorophores that depend on the excitation source in the same way. If the one fluorescent signal is divided by the other, the excitation source information is cancelled and the only information left in the resulting DELIF ratio image is the fluid film thickness<sup>11</sup>. In our CMP DELIF system, the two fluorophores are the polishing pad (polyurethane has a natural fluorescence when exposed to UV light), and Calcein, a dye that is dissolved into the slurry. Figure 1 shows the slurry signal divided by the pad signal for a wafer with etched square wells on top of a Freudenberg FX9 polishing pad. It is clear in the pad image in figure 1 that there is uneven fluorescence excitation. The ratio image on the right side of figure 1 does not contain excitation source information. Further discussion of the DELIF technique will be presented in the “Experimental” section.

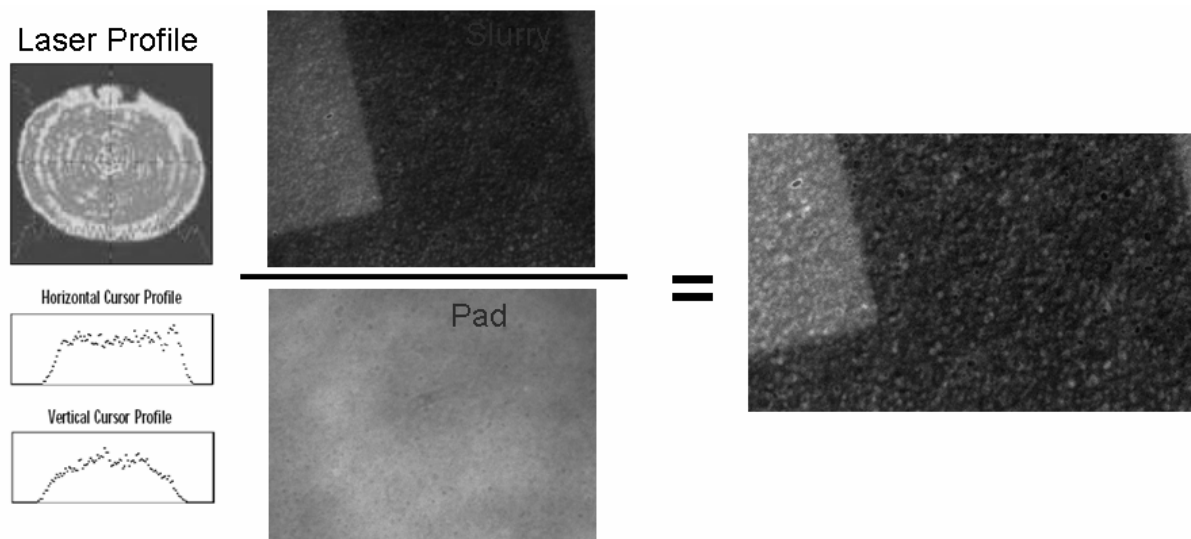


**Figure 1.** Division of the image of the slurry layer by the image of the polishing pad cancels the incident laser light intensity.

The goal of this paper is to use these images to determine pad-wafer contact. Contact in a DELIF image can simply be determined by examining where the slurry layer thickness goes to zero. If a significant amount of contact is present in a DELIF ratio image, there will be significant number of low intensity pixels<sup>8</sup>. We will examine three points on a Cabot Microelectronics D100 (CMC D100) polishing pad and the response of this pad to static pressure loading.

## EXPERIMENT

Figure 2 is a schematic representation of our laboratory scale polisher, a modified RotoPol-31 table top polisher with a 12" platen. The shaft is driven by a 0.5 HP motor. The wafer and the carrier head have been replaced by a 3" diameter, 0.5" thick optical BK7 glass disk such that DELIF measurements are possible. The polishing slurry is a 9:1 water dilution of the Cab-O-Sperse SC1 slurry, containing 3 wt% fumed silica particles. The overly diluted slurry is used to suppress MRR so that experimental boundary conditions are maintained over the course of experimental runs. A water soluble fluorescent dye, Calcein, is dissolved into the slurry at a concentration of 0.5 g/L.

Three interrogation regions along the wafer track were imaged using DELIF. These images were taken without motion of the pad and wafer, i.e. under "static" conditions. Before imaging, slurry was placed onto the pad and the pad was rotated at 20rpm to work the slurry under the wafer and into the pad. Ten images were taken of each spot and the resulting contact images are a sum of those 10 images under 5 different pressure conditions. The first set of 10 images was taken with no additional weight on the shaft. The shaft weighs approximately 2lbs, corresponding to a wafer load of 0.28psi. The weight on the shaft was incremented by 5lbs added to the top of the shaft for each data point, up to 20lbs. The resulting equivalent pressures were as follows: 0.28psi, 1.0psi, 1.7psi, 2.4psi, and 3.1psi. After the images at 3.1psi were taken, the weight was removed from the shaft and another set of 10 images were taken with a 0.28psi load on the wafer.

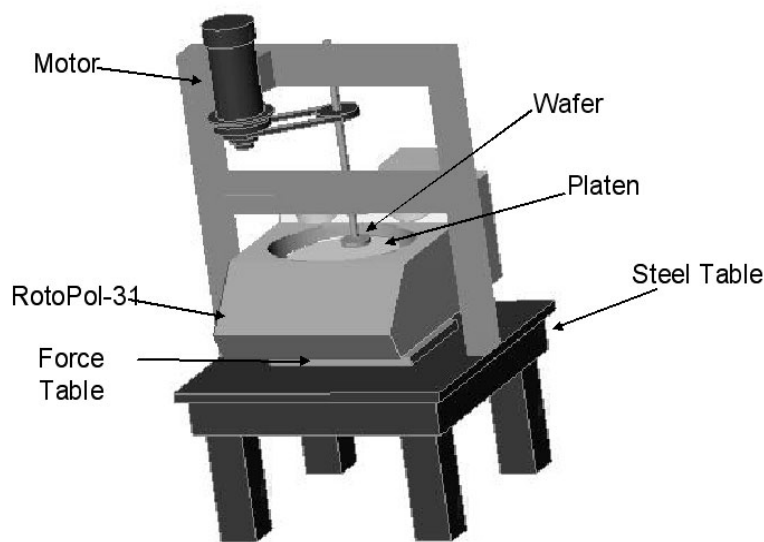


**Figure 2.** Laboratory scale polishing setup.

## **DELIF**

The DELIF system uses the ratio of two different wavelength bands to estimate contact (for a complete DELIF overview see [8]). As illustrated in figure 3, a Nd/YAG laser firing at its third harmonic frequency, 355nm, is used as the excitation source for the high energy fluorophore, the polyurethane pad. The pad emits a fluorescent signal with a peak near 428nm. The Calcein dye dissolved in the slurry absorbs some of the incident laser light, but the majority of the Calcein excitation is from absorption of the pad emission. The Calcein fluoresces with a peak near 530nm. All emitted light from the pad and the Calcein pass through a magnification lens at the end of a long lens tube and into an optics box. The optics box contains a dichroic beam splitter that transmits all wavelengths greater than 475nm and reflects wavelengths less than 475nm. The light entering camera A in figure 3 is the slurry fluorescence and is further filtered by a band pass filter from 540-570nm. The light in camera B containing information about the pad fluorescence passes through an additional band pass filter such that the image contains wavelengths between 385-435nm.

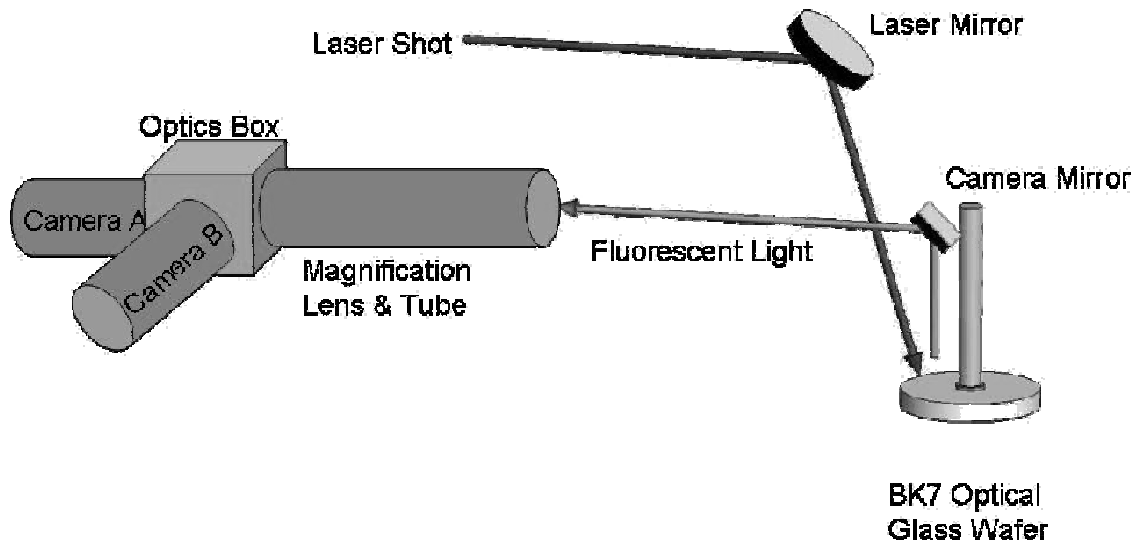


**Figure 3.** DELIF optical setup for acquiring images.

Repeatable calibration of DELIF image intensity to fluid layer thickness has large uncertainties due to several sources of error. These uncertainties are also difficult to quantify. First, errors in alignment of the images from the two cameras can produce phantom profile features and reduce image contrast. We can align our images to within 2-4 pixels using a 5-axis positioner for our beam splitter. This alignment error results in slightly lower image resolution for the DELIF ratio images than the image resolution for the two individual cameras. Second, polyurethane pads often burn when exposed to laser light leading to an average decrease in intensity for the camera B over the course of the data run, and a corresponding DELIF image ratio drift. Images from dynamic CMP runs often produce images in both cameras that have greater intensity due to the influx of fresh dyed slurry under the wafer and slower pad burning. Hidrovo et. al., discusses other sources of optical errors<sup>12</sup>. Pad-wafer contact is a slightly easier measurement to make with DELIF and has less uncertainty than a film thickness measurement. For contact measurements, we only need to ensure that the ratio image intensity information does

not correspond in incident light intensity and examine regions where the intensity approaches zero.

For contact measurements between a flat wafer and polishing pad, it is important that the DELIF image intensity values contain only information about the fluid layer thickness and that the incident light intensity in the two images is cancelled after the images are divided as in figure 1. To ensure that the incident light intensity is cancelled, we can construct a DELIF model for CMP of the light paths passing through a column of fluid that would be detected by a single pixel sensor in the CCD cameras, shown in figure 4.  $I_0$  is the incident laser light,  $I_e$  is the remaining laser excitation light inside the fluid,  $I_p$  is the pad fluorescence, and  $I_d$  is the dye fluorescence. The “+” and “-” superscripts indicate the direction of the light path with respect to the +x axis. The mathematical model takes the form of 6 coupled first-order differential equations:

$$\begin{bmatrix} \dot{I}_e^+ \\ \dot{I}_e^- \\ \dot{I}_p^+ \\ \dot{I}_p^- \\ \dot{I}_d^+ \\ \dot{I}_d^- \end{bmatrix} = \begin{bmatrix} -k_1 & \mu & 0 & 0 & 0 & 0 \\ -\mu & k_1 & 0 & 0 & 0 & 0 \\ 0 & 0 & -k_2 & \mu & 0 & 0 \\ 0 & 0 & -\mu & k_2 & 0 & 0 \\ k_4 & k_k & k_5 & k_5 & -k_3 & \mu \\ -k_4 & -k_4 & -k_5 & -k_5 & -\mu & k_3 \end{bmatrix} \cdot \begin{bmatrix} I_e^+ \\ I_e^- \\ I_p^+ \\ I_p^- \\ I_d^+ \\ I_d^- \end{bmatrix} \quad (1)$$

where  $k_i$  ( $i=1..5$ ) are constants containing absorption and emission behavior, and  $\mu$  is a constant containing scattering behavior. To solve this set of differential equations for the simplest case, we can state the boundary conditions at  $x=0$  for the +x direction and at  $x=L$  for the -x direction, where  $L$  is the total thickness of the column of fluid. The 6 boundary conditions are: the excitation light intensity at  $x=0$  is  $I_0$ ,  $I_e^+(0) = I_0$ ; the pad intensity at  $x=L$  is the fluorescence due to the remaining excitation energy at  $x=L$ ,  $I_p^-(L) = I_e^-(L)\alpha\phi_p$ , where  $\alpha$  and  $\phi_p$  are the absorption and emission constants for the polishing pad, respectively; all other boundary values can be approximated as zero,  $I_e^-(L) = I_p^+(0) = I_d^+(0) = I_d^-(L) = 0$ .

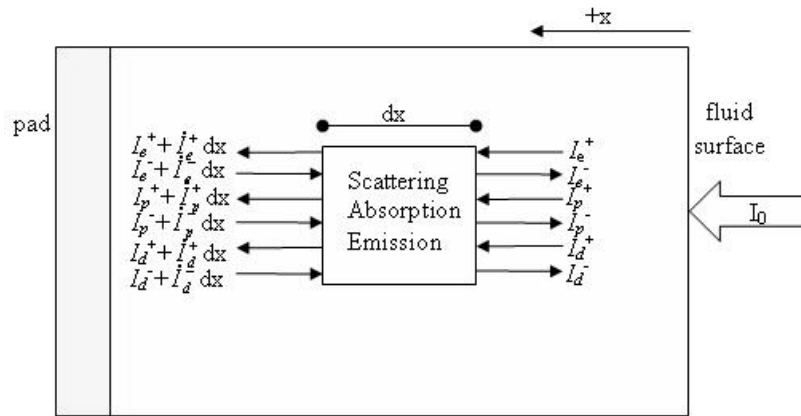


**Figure 4.** Optics Model of DELIF System Used to Acquire Images during CMP.

The final DELIF ratio,  $R$ , is constructed using only the Calcein,  $I_d$ , and the pad,  $I_p$ , fluorescence at zero in the  $-x$  direction:

$$R = \frac{I_d^-(0)}{I_p^-(0)} \quad (2)$$

Although the solution to this model is quite complicated, one can show that  $I_d^-(0)$  and  $I_p^-(0)$  both depend on  $I_0$  such that the incident light information is cancelled from the image, and we should be able to attain DELIF images in which the intensity only depends on fluid layer thickness.

### **Data Acquisition and Processing**

Each DELIF image has the dimensions of 520x696 (361,920) pixels, corresponding to an area of 1.30mmx1.74 mm (2.26mm<sup>2</sup>). The points of contact must be greater in size than the resolution of our imaging system, 2.5  $\mu$ m/pixel, in order to detect contact. If the pixel intensities in the DELIF ratio image are placed into a histogram, we can examine the probability density function (pdf) of the pad heights in each image to detect pad-wafer contact at the low intensity extreme where the fluid layer thickness approaches zero. The region around the maximum value of the pdf is often non-Gaussian<sup>13</sup>. The shape of the high intensity extreme of the pdf represents the pad pore structure<sup>14</sup>. The low intensity extreme of the pdf often has an exponential tail and its shape can reflect the amount of pad conditioning or glazing. If a wafer is placed onto the pad, the tips of the pad asperities should compress and flatten. The resulting DELIF image will contain a larger number of dark pixels where the asperities are flattened, leading to an exponential tail in the low intensity extreme of the pdf. This change in the pdf is due to height equalization at the asperity tips. As contact increases, the number of low intensity pixels also increases leading to a redistribution of the points in the histogram. Effectively, an inflection point will appear in histogram at the low intensity extreme at the point of pad-wafer contact<sup>13,14</sup>. If a significant number of asperities are flattened, a second small peak may even appear in the left side of the image histogram<sup>15</sup>.

Ten images were taken at each applied load for 3 different places on the CMC D100 pad. A histogram with 1000 bins was calculated for each of the 10 DELIF ratio images. Those 10 histograms were averaged to minimize image to image intensity variations. The resulting average histograms for the three spots with a 3.1psi load applied to the shaft and their corresponding DELIF ratio images are shown in figure 5. The lowest intensity bin is bin #0 and the highest intensity bin is bin #1000. All histograms were normalized such that the total area under the histogram is 1. Once a contact threshold is determined, a contact percentage for the image can easily be determine using the normalized histogram by summing the area under the curve to the left of the contact threshold. The y-axis (normalized counts) represents the normalized number of pixels in each intensity bin. The normalized counts are plotted on a logarithmic scale to exaggerate the behavior of the curve at the low intensity extreme. After establishing a contact threshold, a binary threshold can be applied to the original DELIF ratio image and asperity contact regions can be visually identified.

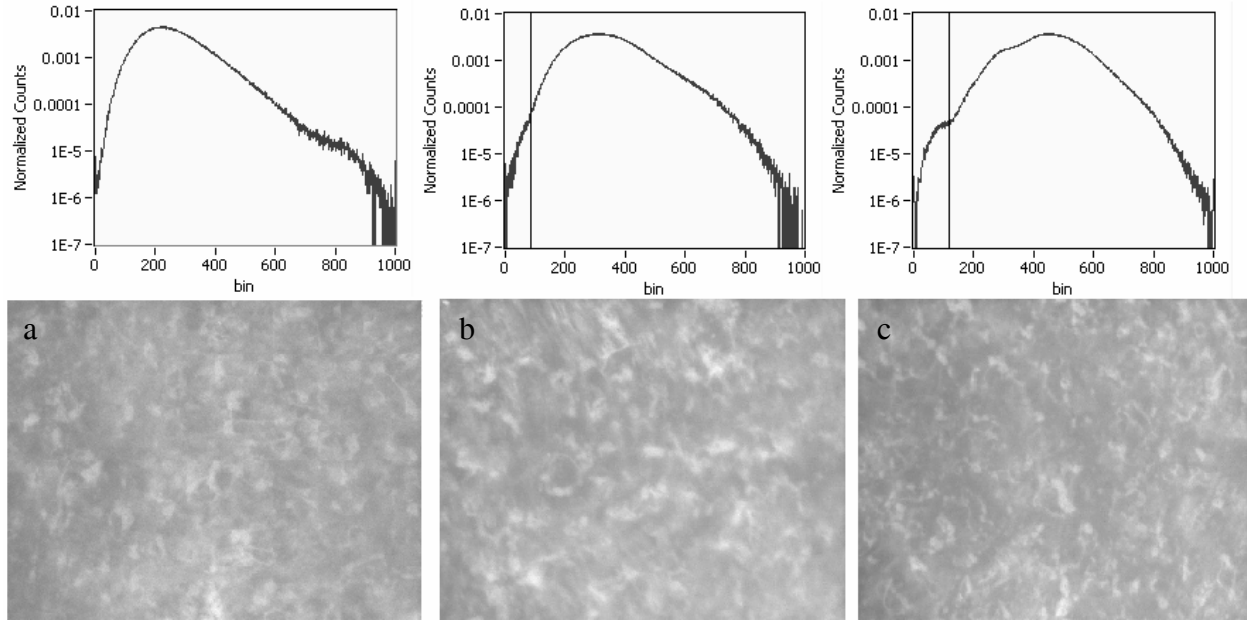


**Figure 5.** Static DELIF images of the CMC D100 polishing pad and their corresponding image histograms. Pad-wafer contact appears in the low intensity side (left) of these histograms as inflection points. (a) There are no inflection points indicating no contact. (b) An inflection point is present at approximately bin 85 indicating contact. (c) Two inflection points are present but only the inflection point located near bin 118 indicates contact because the area under the curve to the left of this threshold increases with pressure.

There is no evidence of pad-wafer contact for image 5a, however, images 5b and 5c do show a pressure dependent region of the histogram to the left of the inflection point. In order to determine if it is possible to attain an image without pad-wafer contact, a 10mm profilometer scan of the polishing pad was taken and is shown in figure 6. The horizontal line at  $+24\mu\text{m}$  on the y-axis indicates the potential position of the wafer resting on the asperity tips. The DELIF imaging width is  $1740\mu\text{m}$ . The profilometer scan in figure 6 contains a 4mm region (from  $3500\mu\text{m}$  to  $7500\mu\text{m}$ ) in which no asperities come into contact with the black horizontal line. Based on this profilometer scan, it seems possible to observe varying amounts of contact and as little contact as 0% with this small interrogation region.

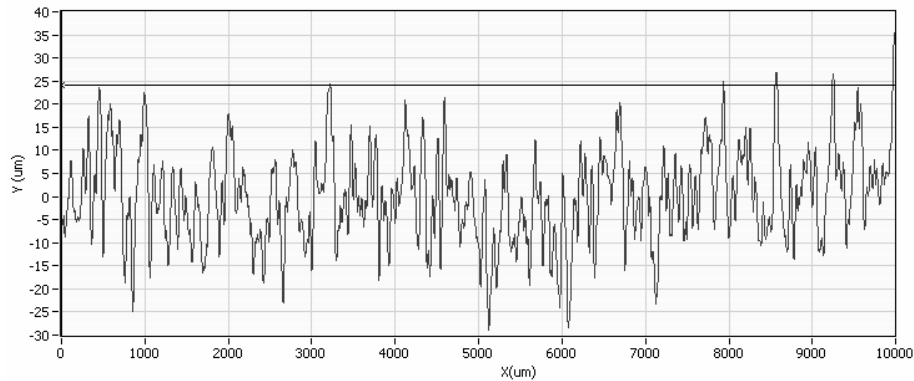


**Figure 6.** A 10mm profilometer scan of the CMC D100 polishing pad. The flat black line indicates the possible position of the wafer on top of this portion of the pad. Few peaks actually come into contact with this line.

## DISCUSSION

Image 5c shows the highest contact percentage. Figure 7 shows the entire pressure series for image 5c. Even at the lowest pressure (0.28psi) there is an inflection point appearing at the low intensity extreme. This histogram has two inflection points to the left of the peak, one near bin #90 and another near bin #250. If contact percentage is calculated at the lower intensity inflection point, there is a clear dependence of contact percentage on pressure. The higher intensity inflection point does not show any dependence on pressure suggesting that this feature does not indicate pad-wafer contact. Calculating the histogram for only the center of image 5c, the inflection point near bin #90 is no longer present, but the inflection point near bin #250 is still present. Both inflection points are eliminated when calculating the histogram for the upper left corner of image 5c and the histogram resembles the histogram for image 5a. These data suggest that we are detecting contact on the left side of image 5c and that the second inflection point may be a property of the polishing pad profile in this portion of the pad.

The data in figure 7 was taken sequentially, starting at 0.28psi adding incremental loads of 0.7psi for each data point up to a maximum load of 3.1psi. The 3.1psi load was then removed from the shaft and another data point was taken at 0.28psi (figure 7f). Figure 8 summarizes the observed contact percentages for images 5c and 5b corresponding to the histograms for each applied pressure. When the 20lb weight was removed from the shaft for image 5c, the histogram did not appear to recover its original shape. The first 0.28psi load yielded a contact of 0.11%, but after the 3.1psi load was removed, the contact percentage remained at 0.28%, most similar to the contact measurement for the 3.1psi case. This may be because the wafer had become suctioned to the pad due to the creation of a low fluid pressure regime induced by the applied weight. All data was taken on an un-grooved pad, which limits slurry flow under the wafer especially in a static rig. However, the same effect was not observed for image 5b; after 20lb weight was removed from the shaft, the contact percentage decreased from 0.17% with 20lbs on the shaft to 0.10%, close to the original contact percentage of 0.07%. In the case of image 5b, the slurry may have been able to seep under the wafer and relieve the fluid pressure gradient and reduce the suction. The variation in the repeatability of the load removal could possibly be due to large scale pad profile variations or variations in the initial placement of the wafer onto the pad.



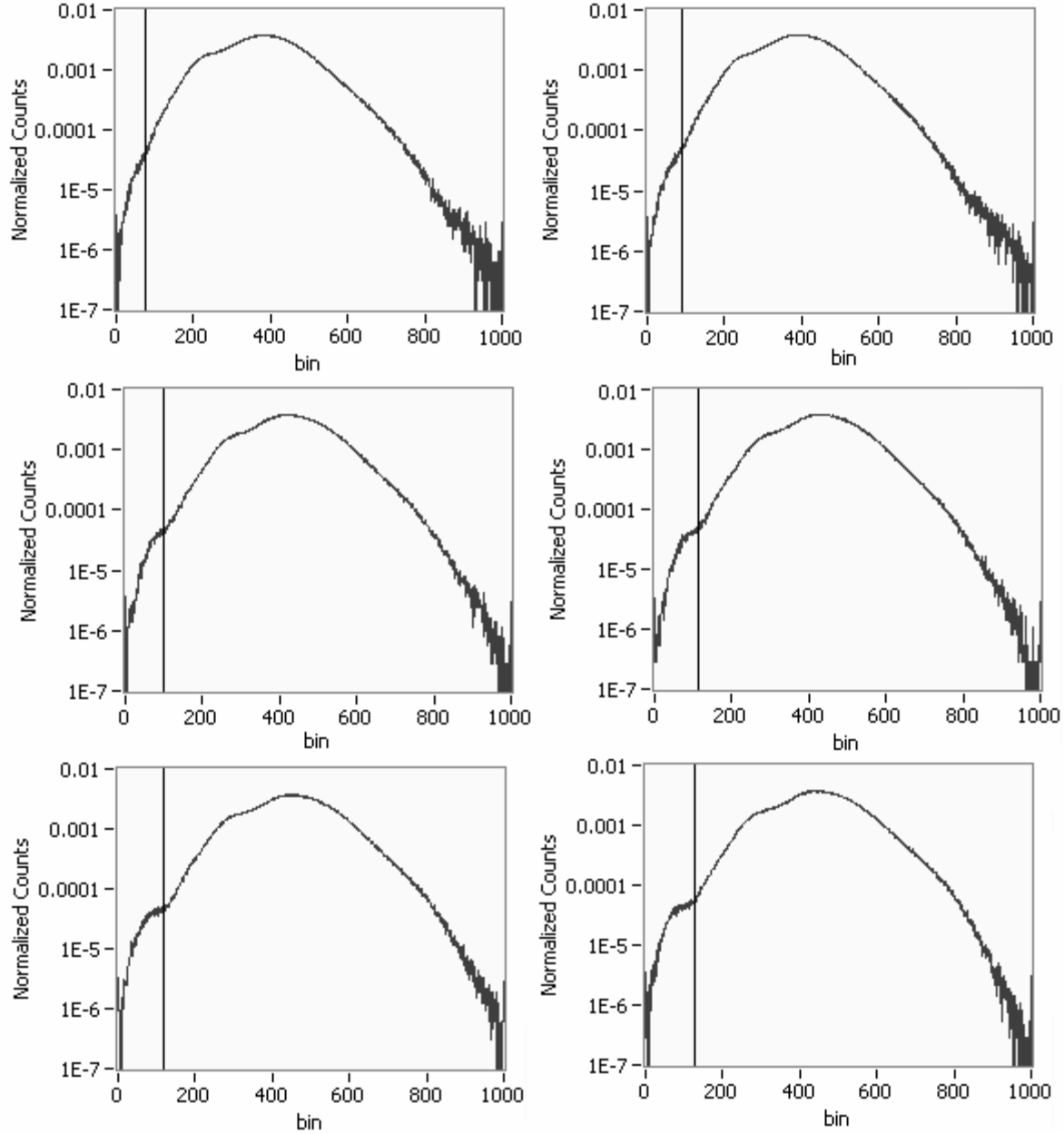


**Figure 7.** Histograms of DELIF image 5c as load is increased. The vertical lines at the first inflection point indicate the contact threshold. The area under the curve to the left of the contact threshold increases with load. (a) 0.28 psi, (b) 1.0 psi, (c) 1.7 psi, (d) 2.4psi, (e) 3.1 psi, (f) histogram of the image after the weight from (e) was removed from the shaft.

The trends present in figures 8a and 8b seem to be linear but this observation should be taken with some caution. There are no error bars on the data points in figure 8 because it is difficult to attain an accurate measure of uncertainty. The point of contact was determined by qualitatively examining the low intensity extreme of the pdf and choosing a contact threshold. Repeated attempts at choosing a threshold yielded variation in the contact percentages of a couple hundredths of a percent, which is enough to affect the observed linearity or sub-linearity in the data. In addition, repeatability of the manner in which weight was added to the shaft is

difficult to control. All attempts were made to place additional weight onto the shaft gently between runs. However, if the pad-wafer suction effect is present and the shaft was pressed slightly harder than the addition of 5lbs to the shaft between runs, we may see contact resulting in a greater effective pressure than originally intended.

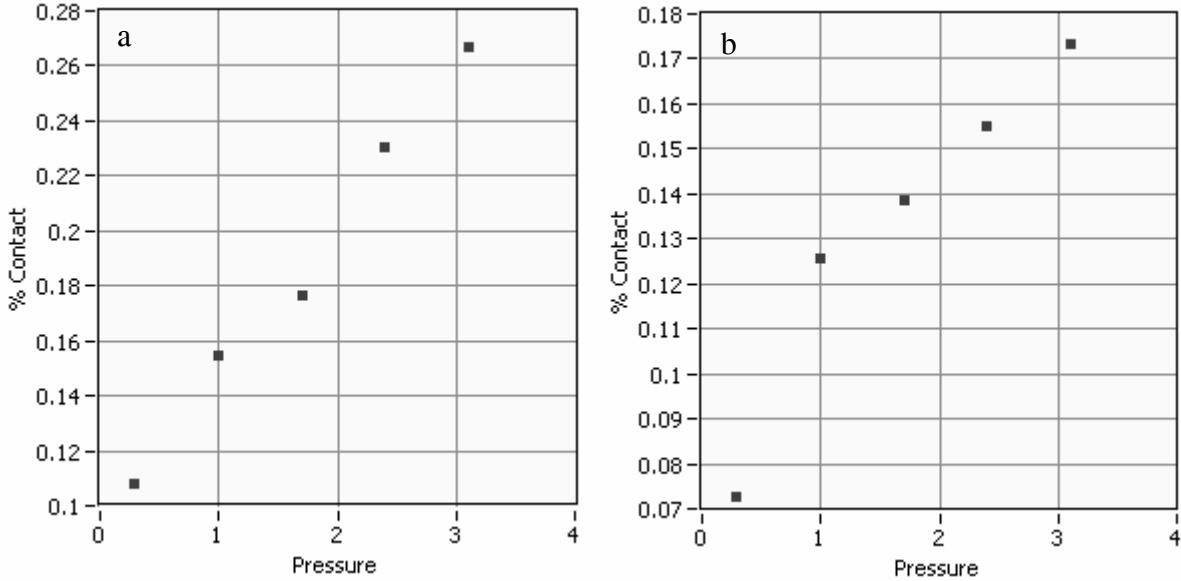


**Figure 8.** (a) Pressure (psi) versus contact percentage for image 5c. (b) Pressure (psi) versus contact percentage for image 5b

Figure 9 shows the contact images corresponding to figure 5c at 0.28psi, 1.7psi and 3.1psi. Asperity contact is indicated by the white parts of the image. For these images, all 10 of the DELIF ratio images at a particular pressure were considered. The threshold was determined in a histogram for each DELIF ratio image. Then, a binary threshold was performed on each image to attain 10 contact images. Those 10 contact images were then summed to produce the images in figure 9. Therefore, the images in figure 9 are 10 level grayscale images where white represents contact appearing in all 10 images of the run and black represents lack of contact appearing in all 10 images of the run.

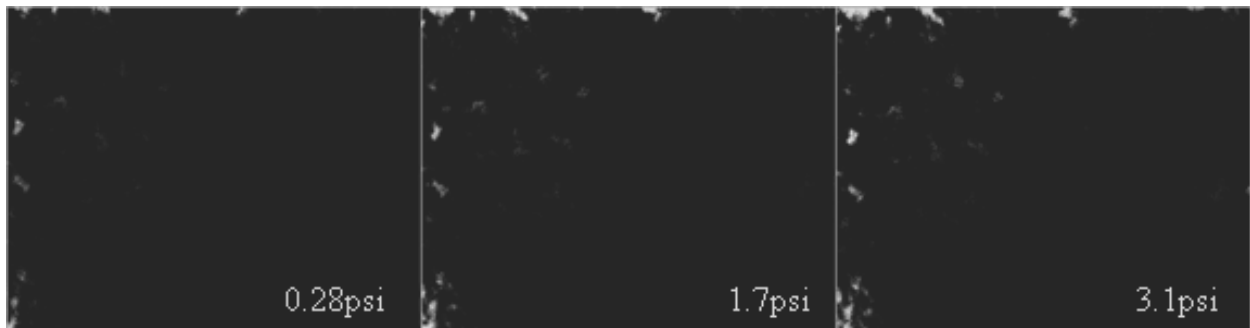


**Figure 9.** Contact images for DELIF image 5b.

Figure 10a shows a region of image 5b with little or no contact at 0.28psi.

As pressure is increased to 1.7 psi, 4 asperities begin to appear in the contact image. Those same 4 asperities are even more clearly visible at 3.1 psi. Image 5a appears to be one of the deeper valleys in the pad because even at 3.1 psi, there is no apparent contact threshold. While image 5c did have the highest contact percentage of the 3 images, most of the contact was localized to the lower left corner of the image. The largest asperity contact region is shown in figure 10b. Since this contact region is in the far corner of the image, it is unclear whether or not the asperity contact area is increasing or if the image is shifting a few microns between data sets as weight is added to the shaft. It is most likely that we are seeing a combination of both effects. If the majority of the contact in an image is near the edge of the images, it may be unclear as to how much of an increase in contact percentages is due to pressure increases or asperities shifting by a few microns from outside the image to inside the image.

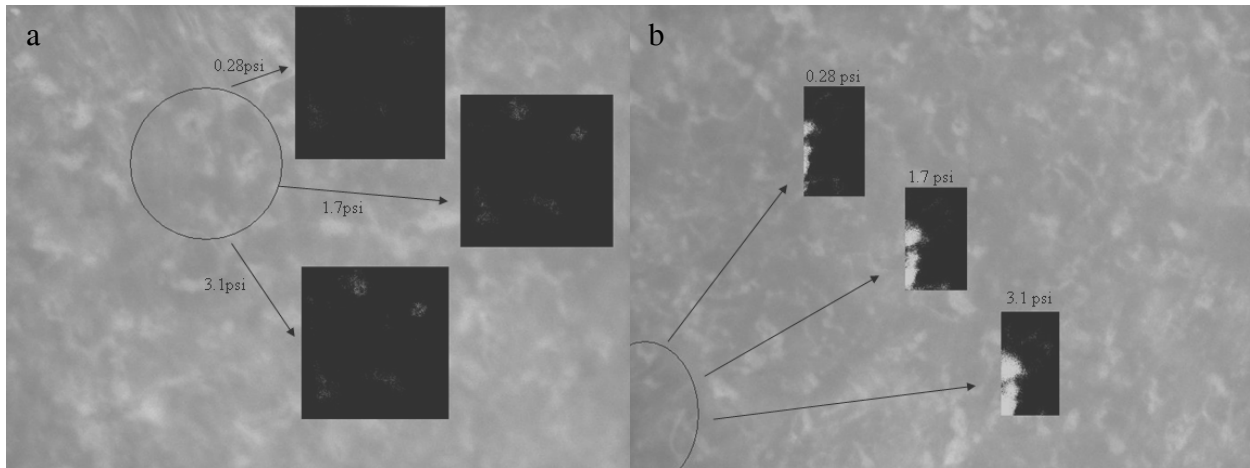


**Figure 10.** (a) A contact region for DELIF image 5b. Four asperities come into contact with the wafer as load is increased from 0.28psi to 3.1psi. (b) A contact region for DELIF image 5c. Contact area increases with pressure.

## CONCLUSIONS

We have presented a technique that employs DELIF for determining pad-wafer contact during polishing. In order to attain accurate contact data from a DELIF ratio image, it is not necessary to calibrate the image intensity to an actual thickness value. However, it is important to cancel the effects of the incident excitation intensity such that the pixel intensities only correspond to a fluid layer thickness. An intensity value from the DELIF image pdf can be chosen as a contact threshold and pad-wafer contact images can be constructed using the threshold value. Summing the area under the pdf to the left of the contact threshold yields a contact percentage for that image. Contact percentages over our imaging region of 1.30x1.74mm vary from 0% to 0.28% on a CMC D100 polishing pad with pressures varying from 0.28psi to 3.1psi. If an image is showing contact at an applied pressure 0.28psi, that contact percentage will increase with pressure. The corresponding contact area for each asperity also increases with pressure. If an image does not show contact, increasing the applied pressure will not necessarily produce contact. All data presented in this paper were taken under static operating conditions. However the methodology can be extended to making measurements during dynamic polishing conditions. These in-situ dynamic contact measurements are currently underway.

## ACKNOWLEDGMENTS

We would like to thank Intel Corporation, Cabot Microelectronics Corporation, and NSF/SRC for providing funding for this project. In addition we would like to thank Len Borucki for his consultation on data analysis.

## REFERENCES

1. J. Yi, *IEEE Trans. Sem. Man.*, **18** (3), 359, (2005).
2. L. M. Cook. *J. of Non-Crys. Solids*, **120**, 152 (1990).
3. E. Paul. *J. Electrochem. Soc.*, **148** (6), G355 (2001).
4. R. P. Glovnea, A. K. Forrest, A. V. Olver and H. A. Spikes. *Trib. Let.*, **15** (3), 217, (2003).
5. G. P. Muldowney, C. L. Elmufdi, R. Palaparthi, D. P. Tselepidakis, S. G. Natu, and V. Vikas. (CMP-MIC Proc., Freemont, CA, 2006) pp. 262-271.
6. C. L. Elmufdi, G. P. Muldowney. "The Impact of Pad Microtexture and Material Properties on Surface Contact and Defectivity in CMP", *11<sup>th</sup> International CMP Symposium, Lake Placid, NY*, 2006.
7. C Gray, D Apone, C Rogers, V P Manno, C Barns, M Moinpour, S Anjur, and A Philipossian. *Electrochem. Solid State Let.* **8**, G109, (2005).
8. D Apone, C Gray, C Rogers, V Manno, C Barns, M Moinpour, S Anjur, and A Philipossian. (Mater. Res. Soc. Proc. 867, San Francisco, CA, 2005) pp. W2.3.
9. C Gray, D Apone, C Barns, M Moinpour, S Anjur, V Manno, and C Rogers. (Mater. Res. Soc. Proc. 867 San Francisco, CA, 2005), pp. W5.4.
10. J Coppeta and C Rogers. *Exp. in Fluids*, **25**, 1, (1998).
11. C. H. Hidrovo and D. P. Hart. *Meas. Sci. & Tech.*, **12**, 467, (2001).
12. C. H. Hidrovo, R. R Brau, and D. P. Hart. *Applied Optics*, **43** (4), 894, (2004).
13. L. Borucki. (private communication, March 2007).
14. L. Borucki, T. Witelski, C. Please P. Kramer and D. Schwendeman. (CAMP Symposium 13, Lake Placid, NY, 2003).
15. A. S. Lawing. (5<sup>th</sup> Int. Symp on CMP, Philadelphia, PA, 2002).